European Journal of Cell Biology 94 (2015) 148–161

Contents lists available at ScienceDirect

European Journal of Cell Biology

journal homepage: www.elsevier.com/locate/ejcb

Loss of lysosome-associated membrane protein 3 (LAMP3) enhances cellular vulnerability against proteasomal inhibition

Jorge Antolio Dominguez-Bautista[a], Michael Klinkenberg[a], Nadine Brehm[a], Mahalakshmi Subramaniam[b], Beatrice Kern[b], Jochen Roeper[b], Georg Auburger[a], Marina Jendrach[a,*]

[a] Experimental Neurology, Department of Neurology, Goethe University Medical School, Frankfurt am Main, Germany
[b] Institute of Neurophysiology, Goethe University Medical School, Frankfurt am Main, Germany

ARTICLE INFO

Article history:
Received 25 August 2014
Received in revised form
26 December 2014
Accepted 15 January 2015

Keywords:
Autophagy
Cancer
LAMP3
Lysosome
Parkinson's disease
Proteasome

ABSTRACT

The family of lysosome-associated membrane proteins (LAMP) includes the ubiquitously expressed LAMP1 and LAMP2, which account for half of the proteins in the lysosomal membrane. Another member of the LAMP family is LAMP3, which is expressed only in certain cell types and differentiation stages. LAMP3 expression is linked with poor prognosis of certain cancers, and the locus where it is encoded was identified as a risk factor for Parkinson's disease (PD). Here, we investigated the role of LAMP3 in the two main cellular degradation pathways, the proteasome and autophagy. *LAMP3* mRNA was not detected in mouse models of PD or in the brain of human patients. However, it was strongly induced upon proteasomal inhibition in the neuroblastoma cell line SH-SY5Y. Induction of *LAMP3* mRNA following proteasomal inhibition was dependent on UPR transcription factor ATF4 signaling and induced autophagic flux. Prevention of *LAMP3* induction enhanced apoptotic cell death. In summary, these data demonstrate that *LAMP3* regulation as part of the UPR contributes to protein degradation and cell survival during proteasomal dysfunction. This link between autophagy and the proteasome may be of special importance for the treatment of tumor cells with proteasomal inhibitors.

Introduction

The ubiquitin-proteasome system and the autophagic-lysosomal pathway are the two major degradation systems for proteins in eukaryotic cells. They are responsible for the degradation of unnecessary, dysfunctional or damaged components, from soluble proteins to protein aggregates and whole organelles (Korolchuk et al., 2010). The ubiquitin-proteasome system mediates the enzymatic ubiquitination of substrate proteins. The tagged proteins are then recognized by a barrel-shaped structure called the proteasome, in which they are degraded to peptides (Glickman and Ciechanover, 2002). Autophagic-lysosomal degradation can be classified into macroautophagy, chaperone mediated autophagy and microautophagy. In macroautophagy (usually referred to as autophagy) the substrate cargo is engulfed by the autophagosome, which is characterized by the presence of the protein LC3-II. Once the cargo is completely surrounded by the autophagosome, this double-membrane organelle fuses with the lysosome, where proteolysis occurs (He and Klionsky, 2009; Mizushima, 2007).

The ubiquitin-proteasome system and autophagy do not act independently from each other. Defective autophagy results in accumulation of ubiquitinated proteins, impacting the flux of the ubiquitin proteasome system. On the other hand, dysfunction of the proteasome can promote a compensatory induction of autophagy (Korolchuk et al., 2010; Nedelsky et al., 2008).

Lysosomal function depends on lysosomal hydrolases and integral lysosomal membrane proteins. Over 25 lysosomal membrane proteins are known, which participate in diverse tasks such as lysosomal acidification, membrane fusion and transport of degradation products to the cytoplasm (Saftig and Klumperman, 2009). The family of lysosome-associated membrane proteins (LAMP) includes

Abbreviations: CCCP, carbonyl cyanide m-chlorophenyl hydrazone; DMSO, dimethyl sulfoxide; FCS, fetal calf serum; GFP, green fluorescent protein; HBSS, Hank's Balanced Salt Solution; LAMP, lysosome-associated membrane protein; LC3, microtubule-associated protein light chain 3; PARP, poly ADP ribose polymerase; PD, Parkinson's disease; ROI, region of interest; UPR, unfolded protein response.

* Corresponding author. Current address: Institut für Neuropathologie Charité - Universitätsmedizin Berlin Campus Charité Mitte Charitéplatz 1 | Virchowweg 15, D-10117 Berlin, Germany. Tel.: +49 30 450 536291.
E-mail address: marina.jendrach@charite.de (M. Jendrach).

http://dx.doi.org/10.1016/j.ejcb.2015.01.003
0171-9335/

five members: LAMP1, LAMP2, LAMP3, BAD-LAMP and macrosialin (CD68/LAMP4), which share a so-called LAMP domain and possess several N- and O-glycosylation sites (Saftig et al., 2010; Wilke et al., 2012).

LAMP1 and LAMP2 represent about 50% of the lysosomal membrane proteins (Saftig et al., 2010). They are type-1 transmembrane proteins with high sequence homology, containing a highly glycosylated luminal domain and a short cytosolic tail (Saftig and Klumperman, 2009). The generation of LAMP1 knockout mice resulted in mild regional brain astrogliosis and upregulation of LAMP2 at the protein level. However, the distribution and density of lysosomes, as well as lysosomal enzyme activity, pH and osmotic stability were unaffected (Andrejewski et al., 1999). On the other hand, LAMP2 knockout mice showed increased mortality between 20 and 40 days of age, with the surviving mice being fertile and having a normal life span, although they showed accumulation of autophagic vacuoles in several tissues (Tanaka et al., 2000). A LAMP1/LAMP2 double knockout resulted in embryonic death between E14.5 and E16.5. Fibroblasts derived from those double knockout embryos showed accumulation of autophagic vacuoles and of LC3-II after amino acid starvation, indicating impairment of autophagic flux (Eskelinen et al., 2004).

Unlike the ubiquitous LAMP1 and LAMP2, LAMP3 (also called DC-LAMP, CD208, or TSC403) is expressed only in specific tissues and conditions. Early reports on LAMP3 showed that it is induced upon human dendritic cell differentiation (de Saint-Vis et al., 1998), that it is present in normal and transformed human type II pneumocytes (Akasaki et al., 2004; Salaun et al., 2004), and is increased in carcinomas of different origin, where it has been linked to metastasis of tumor cells and poor prognosis (Kanao et al., 2005; Ozaki et al., 1998).

Additionally, despite the lack of evidence for LAMP3 expression in brain tissue (Akasaki et al., 2004; de Saint-Vis et al., 1998), several genome-wide association studies have identified the chromosomal locus *MCCC1/LAMP3* associated with increased risk for sporadic old-age Parkinson's disease (PD) (Li et al., 2013; Lill et al., 2012; Pihlstrom et al., 2013). Finally, LAMP3 was shown to be involved in the unfolded protein response (UPR) during hypoxia (Nagelkerke et al., 2013a), while its localization points to a possible function in autophagic-lysosomal degradation.

As recent data indicate that the autophagic-lysosomal pathway and the ubiquitin-proteasome system act together to maintain protein homeostasis (Korolchuk et al., 2010; Park and Cuervo, 2013; Vogl et al., 2014), we evaluated the hypothesis that *LAMP3* represents a link between these two systems.

Materials and methods

Cell culture

HeLa cells were cultured in Minimal Essential Medium with Earle's salts (Gibco) supplemented with 1× MEM Non-Essential Aminoacids (Gibco), 10% FCS Gold (PAA), and 10 mM HEPES buffer 10 mM (PAA). Neuroblastoma SH-SY5Y cells were cultured in RPMI 1640 medium (Gibco) supplemented with 10% FCS (PAA). Both cell lines were kept at 37 °C, 5% CO_2 and 95% air. SH-SY5Y cells were cultured with the following drugs at the indicated final concentration: U0126 10 μM, LY294002 25 μM, CCCP 10 nM, rapamycin 0.5 μM, staurosporine 30 nM, bafilomycin A1 10 nM, 3-methyladenine 10 mM, MG132 3 μM or 300 nM, epoxomicin 1 μM, thapsigargin 1 μM, and tunicamycin 1 μg/ml. DMSO was included as control at a final concentration of 0.05%. Cells were deprived of amino acids by culturing them in Hank's Balanced Salt Solution HBSS (Gibco). Differentiation of SH-SY5Y cells was performed by culturing cells at a density of 52 000 cells/cm^2 in RPMI medium supplemented with 3% FCS and 10 μM retinoic acid for 10 days. New medium was added every other day.

Infusion of mouse brains with epoxomicin

Infusion of mice midbrains was performed as described elsewhere (Subramaniam et al., 2014). Briefly, 4 μl of epoxomicin (10 μM) or DMSO (1%) were unilaterally injected into the substantia nigra of 11-week old mice. Either 24 h or 2 weeks post-injection, the mice were euthanized. The midbrain (including substantia nigra) of the injected side was immediately dissected, frozen in liquid nitrogen, and stored at −80 °C. Total RNA was isolated using the TRI® reagent, and qRT-PCR analysis was performed as described below.

Post-mortem samples of human brain

Brain tissue samples from autopsy-confirmed subjects with Parkinson's disease with Braak stage 6 ($n = 6$) of α-synuclein pathology and age-/gender-matched controls ($n = 4$, Supplementary Table 1) were obtained from the Neurobiobank Munich with approval of the Frankfurt University Medical school ethics committee. Pathological analysis was performed according to the Lewy Body Dementia staging (Braak et al., 2003). At ages above 60 years, all PD and control cases had some Alzheimer-associated neurofibrillary tangle pathology (Braak and Braak, 1991). The PD cases had confirmed α-synuclein pathology in the cingulate gyrus, while the controls were chosen so that no α-synuclein-, amyloid-beta- or MAP-tau-pathology was detectable in this brain region (Thal et al., 2002). Gray matter from the posterior cingulate gyrus next to the posterior thalamus was dissected for total RNA and protein isolation.

Total protein was obtained from ∼150 mg of tissue by serial isolation. First, the tissue was homogenized with a Dounce tissue grinder (Wheaton) and 10 volumes of RIPA buffer (50 mM Tris–HCl pH 7, 150 mM NaCl, 0.1% SDS, 1% Triton X-100, 0.5% sodium deoxycholate, 2 mM EDTA, and 1× protease inhibitors). Lysate was centrifuged at 9000 × *g* for 10 min at 4 °C and the RIPA-insoluble pellet was then lysed with 2× SDS buffer (137 mM Tris–HCl pH 6.8, 4% sodium dodecyl sulfate, 20% glycerol, 1× protease inhibitors), sonicated for 10 s with a homogenizer (Bandelin) and centrifugated at 9000 × *g* for 10 min. The 2× SDS-soluble fraction contains membrane-associated proteins and was used for LAMP3 western blot. Total RNA was isolated from ∼50 mg of tissue using the TRI® reagent. RNA integrity was determined using the Agilent RNA 6000 Pico Kit and the Agilent 2100 Bioanalyzer (Agilent). Gene expression was measured by qRT-PCR as indicated below.

Plasmid, siRNAs, and cell transfection

A plasmid coding for LAMP3 with enhanced green fluorescent protein fused at the C-terminal end (LAMP3-GFP) was generated by subcloning the open reading frame of human LAMP3 (NM_014398.3) into the XmnI and NotI restriction sites of vector pEZ-M03, under the control of the Cytomegalovirus promoter (GeneCopoeia).

The siRNAs AllStars Negative Control (1027281), Hs_LAMP3_5 (SI041532226), Hs_LAMP3_7 (SI04287458), and Hs_ATF4_5 (SI03019345) from QIAGEN were used.

The Amaxa Cell Line Nucleofector kit V and the Nucleofector™ 2b Device (Lonza) were used to transfect 1.5×10^6 SH-SY5Y cells with 0.1 nmol of siRNAs according to the manufacturer's instructions. Transfection of HeLa cells was performed by plating 250 000 cells on gelatin-coated 24-mm coverslips. Cells were transfected using 1 μg of plasmid with the Effectene kit (QIAGEN) according to manufacturer's instructions.

cDNA synthesis and quantitative RT-PCR

Total RNA from cells was isolated using the RNeasy Mini Kit (QIAGEN) according to manufacturer's instructions. One microgram of total RNA was used for cDNA synthesis using the SuperScript III Reverse transcriptase (Life Technologies). Quantitative Real Time Polymerase Chain Reaction (qRT-PCR) was performed in a Step One Plus Real Time PCR System (Life Technologies) using the following TaqMan assays: *LAMP1* (Hs00931464_m1), *LAMP2* (Hs00903587_m1, which detects the *LAMP2A*, *LAMP2B*, and *LAMP2 C* isoforms), *LAMP3* (Hs01111317_m1), *ATG5* (Hs00355494_m1), *BECN1* (Hs00186838_m1), *ATG7* (Hs00197348_m1), *DDIT3* (Hs00358796_g1), *HSPA5* (Hs99999174_m1), *ATF3* (Hs00231069_m1), *ATF4* (Hs00909569_g1), *SQSTM1* (Hs00177654_m1), *PINK1* (Hs00260868_m1), *PARKIN* (Hs01038318_m1), *ATP13A2* (Hs01119446_m1), *DJ-1* (Hs00697109_m1), *SNCA* (Hs01103386_m1), *ATNX2* (Hs00268077_m1), *EIF4A2* (Hs01115195_g1), *SYT11* (Hs01064643_m1), *CPLX1* (Hs00362510_m1), *NSF* (Hs00938040_m1), *RAB7L1* (Hs01026316_m1), *RAB25* (Hs01040784_m1), *GAK* (Hs01049227_m1), *BST1* (Hs 01070189_m1), *STK39* (Hs01085346_m1), *HIP1R* (Hs00391321_m1), *EIF4A2* (Hs01115195_g1), *GAPDH* (Hs99999905_m1), *TBP* (Hs99999910_m1), *Lamp3* (Mm00616604_m1), and *Tbp* (Mm00446973_m1). *TBP* or *Tbp* were used as human or mouse housekeeping genes, correspondingly. Relative gene expression was calculated using the $2^{-\Delta\Delta Ct}$ formula.

Western blot

Total protein was isolated with 2× SDS lysis buffer (137 mM Tris–HCl pH 6.8, 4% sodium dodecyl sulfate, 20% glycerol, 1× protease inhibitors). The cell lysate was sonicated for 10 s with a homogenizer (Bandelin) and centrifugated at 9000 × *g* for 10 min. Supernatant was collected and protein concentration was determined with a protein quantitation kit (Interchim) using bovine serum albumin as standard. Human lung tissue lysate was obtained from Novus biologicals. 15–30 μg of total protein lysate were separated by SDS-PAGE, transferred to a PVDF membrane, and blocked with 5% skim milk in 1× PBS/0.1% Tween. For analysis of brain tissue, 15 μg of protein were separated using 4–12% Bis–Tris pre-cast gels (Novex). Membranes were probed using the following primary antibodies: LC3 (Sigma), SQSTM1 (Santa Cruz), PARP (Cell Signaling), GFP (Living Colors), and GAPDH (Calbiochem). The following LAMP3 antibodies were used: ab83659 (Abcam), AF4087 (R&D systems), MABC44 (Millipore), and 10527-RP02 (Sino Biological Inc.). Secondary antibodies were conjugated with horseradish-peroxidase, and detection was performed with West pico chemiluminescent Super Signal Substrate. Band intensity was quantified using the ImageJ software.

Protein deglycosylation

Protein lysates were obtained using a deglycosylation lysis buffer (50 mM Tris HCl pH 7.4, 150 mM NaCl, 1% IGEPAL, 0.5% Deoxycholate acid, 0.1 mM EDTA, 1× Protease inhibitor cocktail). 30 μg of protein were used for deglycosylation using PNGase F, which removes N-glycosylation; or with deglycosylation mix, which removes N- and O-glycosylation (New England Biolabs) according to supplier instructions. Molecular weight shifts were analyzed by western blot.

Caspase-3 activity assay

Cells were lysed in caspase-3 lysis buffer (10 mM HEPES pH 7.4, 150 mM NaCl, 1 mM EDTA, 0.5% Chaps, 1 mM Dithiothrietol, 1 μg/ml Pepstatin A, and 1 mM PMSF). Cells were sonicated and the lysate was centrifuged at 9000 × *g* for 10 min. Supernatant was collected and the protein concentration was determined by the Bradford method using bovine serum albumin as reference.

Between 1 and 5 μg of protein were mixed with caspase-3 reaction buffer (25 mM HEPES pH 7.4, 1 mM EDTA, 0.1% Chaps, 1 mM DTT, 10 μM AC-DEVD-AMC, and 8.6% D(+)-Sucrose). Fluorescence intensity was measured every 10 min over the course of 2 h using excitation at 360 nm and emission at 465 nm in a GENios microplate reader (Tecan).

Confocal laser scanning microscopy and immunostaining

Cells were cultured on gelatin-coated coverslips, fixed with 4% paraformaldehyde for 20 min, washed 3 times with phosphate buffered Saline 1× (PBS 1×), permeabilized with 0.1% Triton X-100 for 20 min, washed 3 times with PBS 1×, blocked with 3% bovine serum albumin for 1 h, and incubated overnight with the respective primary antibody: LAMP2/CD107b, which detects the three isoforms of LAMP2 (BD Biosciences), p62/SQSTM1 (Santa Cruz) and LAMP1 (BD Bioscience). Next day incubation with a Cy3-conjugated secondary antibody (Jackson ImmunoResearch) was performed for 2 h and the nucleus was counterstained with Hoechst 33258.

Microscopic analysis was performed using a Leica TCS SP5 confocal laser scanning microscope and a HCX PL APO lambda blue 63× OIL UV objective controlled by LAS AF scan software (Leica Microsystem, Wetzlar, Germany). Images were taken simultaneously and co-localization was determined with the program Fiji (function Coloc2) using single slices and ROIs. The number of lysosomes was determined with the program Fiji as described before (Parganlija et al., 2014). Images in the figures represent maximum image projections.

Data analysis

Experiments were repeated at least 3 times independently. Values are presented as mean ± SEM (Standard Error of the Mean). Statistical difference between means was assessed by the two-tailed Student *t*-test when comparing two groups, and by one-way ANOVA with Bonferroni's *post hoc* test when comparing three or more groups using the GraphPad Prism software. Statistically significant values are indicated by $^{*}p \leq 0.05$, $^{**}p \leq 0.01$, and $^{***}p \leq 0.001$.

Results

LAMP3 is detectable in the neuroblastoma cell line SH-SY5Y but not in brain

Early reports indicate that *LAMP3* mRNA is undetectable in human or mouse brains (Ozaki et al., 1998; Salaun et al., 2003). However, several genome-wide association studies (GWAS) of PD have recently identified the locus *MCCC1/LAMP3* as a risk factor for the disease (Li et al., 2013; Lill et al., 2012; Pihlstrom et al., 2013). Thus, the expression of *Lamp3* was investigated in a mouse model that overexpresses α-synuclein, a crucial protein in the pathogenesis of PD or in control animals with the same genetic background (wild type). This animal model overexpresses the mutant human A53T-α-synuclein under the control of the neuron-specific prion promoter. The animals display normal motor activity at 6 months, but progress to impaired spontaneous movement by 18 months, without detectable neuronal loss in the nigrostriatal projection or protein degradation and aggregation problems (Gispert et al., 2003). Quantitative RT-PCR analysis showed that *Lamp3* was undetectable in cerebellum, hippocampus, striatum, and midbrain of wild type mice between 3 and 20 months old. Similarly, *Lamp3*

Table 1
Lamp3 expression in mouse brain regions. Specific brain regions were dissected, total RNA was isolated and *Lamp3* expression was measured by qRT-PCR.

Genotype or treatment	Tissue	Age or duration of treatment	*n*	*Lamp3* (Ct)[a]	*Tbp* (Ct)[a]
Wild type	Cerebellum	3 months	5	Undetectable	27.35 ± 0.09
	Hippocampus	20 months	3	Undetectable	27.76 ± 0.01
	Striatum	6 months	6	Undetectable	27.10 ± 0.06
	Striatum	20 months	6	Undetectable	27.52 ± 0.10
	Midbrain	6 months	6	Undetectable	27.78 ± 0.07
	Midbrain	20 months	6	Undetectable	28.18 ± 0.02
A53T-α-synuclein	Striatum	20 months	6	Undetectable	27.32 ± 0.09
	Midbrain	6 months	6	Undetectable	27.64 ± 0.12
	Midbrain	20 months	6	Undetectable	28.00 ± 0.08
DMSO	Midbrain	24 h	4	Undetectable	27.71 ± 0.12
Epoxomicin	Midbrain	24 h	4	Undetectable	27.61 ± 0.06
DMSO	Midbrain	2 weeks	4	Undetectable	27.42 ± 0.04
Epoxomicin	Midbrain	2 weeks	4	Undetectable	27.51 ± 0.04
Mouse lung[b]			1	25.03	32.11

[a] Ct values of *Lamp3* and *Tbp* were determined by qRT-PCR using mouse-specific *Lamp3* TaqMan probes.
[b] Expression of *Lamp3* in mouse lung is shown for comparative purposes.

Table 2
Ct values of *LAMP genes* in SH-SY5Y cells. Total RNA was isolated from cells in control conditions and genes were detected by qRT-PCR.

Gene	Ct values[a]
TBP	26.54 ± 0.68
LAMP1	24.03 ± 0.10
LAMP2	27.23 ± 0.81
LAMP3	32.24 ± 0.54

[a] Ct values were obtained by qRT-PCR in at least 3 independent measurements.

mRNA was undetectable in striatum or midbrain of 6- and 20-month-old transgenic mice (Table 1).

Since the GWAS are based on human probands, the expression of LAMP3 was investigated in post-mortem brain tissue of PD cases and age-/gender-matched controls. Braak staging indicated that PD cases were in stage 6 (Table S1), showing substantial Lewy body and neurite pathology in the cingulate gyrus. Despite low RNA integrity due to postmortem time, qRT-PCR could be successfully performed for the housekeeping genes *EIF4A2*, *GAPDH*, and *TBP*. Nevertheless, analysis of *LAMP3* showed average Ct values of ~37, close to a non-specific signal (Fig. S-1A). Accordingly, comparing the levels of *LAMP3* in PD cases *versus* controls showed no differences (Fig. S-1B). To determine whether the LAMP3 protein was present, western blot analysis was performed. PD samples and controls showed a strong GAPDH signal, but no detectable LAMP3 protein (Fig. S-1C). These data indicate that LAMP3 is not expressed in the mouse brain or in the human cingulate gyrus, even when PD pathology is present.

Tumor transformation is a factor that correlates with *LAMP3* expression (Kanao et al., 2005; Ozaki et al., 1998). To determine whether *LAMP3* is present in brain cancer cells, the expression of *LAMP1*, *2*, and *3* was determined in human neuroblastoma SH-SY5Y cells by qRT-PCR. Table 2 shows that *LAMP1* and *LAMP2* are expressed strongly in SH-SY5Y cells, with Ct values comparable to those of the housekeeping gene *TBP*. In contrast, *LAMP3* displays Ct values that reflect relatively low expression, but still significantly above non-specific signals (Ct values >35). This analysis indicates that *LAMP3* is present in neuroblastoma cells, probably due to its tumorigenic nature as reported for other cell lines (Kanao et al., 2005; Nagelkerke et al., 2011; Pennati et al., 2013).

LAMP3 and LAMP2 colocalize in the perinuclear area but not in the cellular periphery

The different phenotypes of knockout mice lacking either LAMP1 (Andrejewski et al., 1999) or LAMP2 (Tanaka et al., 2000), and the cell-specific expression pattern of LAMP3 (de Saint-Vis et al., 1998; Kanao et al., 2005; Ozaki et al., 1998) suggest that these proteins have distinct functions. Thus, the subcellular localization of LAMP3 and LAMP2 was compared. A LAMP3-GFP fusion protein was generated and transiently expressed in HeLa cells; one day after transfection LAMP2 was visualized by antibody staining and the co-localization of both proteins was determined by confocal scanning microscopy. The images show that LAMP3-GFP colocalizes with LAMP2 with a mean Pearson correlation coefficient of 0.78. This occurs mostly in the perinuclear area, while in the cellular periphery a significant number of vesicles are only positive for either LAMP3-GFP or LAMP2 (Fig. 1A).

A common characteristic of the LAMP family members is their posttranslational glycosylation. The expected primary size of LAMP3-GFP without posttranslational modifications is ~70 kDa. Western blot analysis of LAMP3-GFP lysates using an anti-GFP antibody detected two bands: the main band at ~90 kDa, and a weaker band at ~130 kDa. In deglycosylated samples, LAMP3-GFP immunoreactivity appeared also in two bands, at ~70 kDa and ~110 kDa, indicating a deglycosylation size shift of ~20 kDa (Fig. 1B). These results indicate that LAMP3 exists with different degrees of posttranslational modification: 20 kDa due to posttranslational glycosylation and an additional modification of 40 kDa of unknown nature. In summary, these results suggest that the LAMP proteins share posttranslational glycosylation, but their partially overlapping intracellular localization (Fig. 1A) and differential tissue expression (de Saint-Vis et al., 1998; Kanao et al., 2005; Ozaki et al., 1998; Saftig et al., 2010) suggest distinct functional roles.

LAMP3 is strongly induced by proteasomal inhibition in neuroblastoma cells

To determine the functional role of LAMP3, several stimuli and stressors were used to determine their influence on *LAMP3* expression in neuroblastoma SH-SY5Y cells. Measurement of transcript levels showed that the following stimuli resulted in the downregulation of *LAMP3*: retinoic acid-induced differentiation, inhibition of the MEK/ERK pathway with U0126, inhibition of the PI3K/Akt pathway with LY294002, mitochondrial uncoupling with CCCP, as well as induction of autophagy by the mTOR inhibitor rapamycin or serum-/amino acid deprivation with HBSS medium. In contrast, staurosporine did not affect *LAMP3* mRNA expression significantly. The following stressors promoted the induction of *LAMP3*: blockage of autophagy with the V-ATPase inhibitor bafilomycin A1 or the PI3K inhibitor 3-methyladenine, and inhibition of the proteasome with MG132 or epoxomicin (Fig. 2A). The upregulation of *LAMP3*

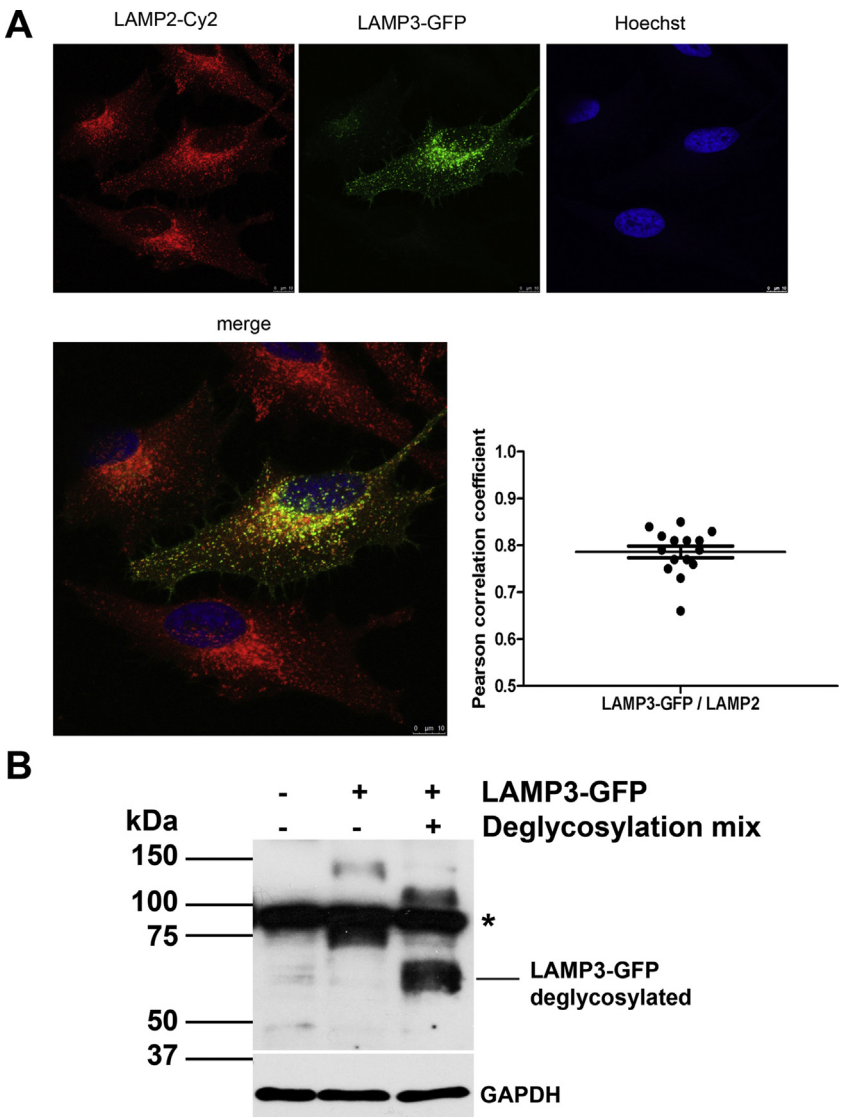

Fig. 1. Differential localization of LAMP3 and LAMP2. (A) HeLa cells were transfected with the plasmid LAMP3-GFP (green) and one day after transfection stained with an anti-LAMP2 antibody (red). LAMP3-GFP showed colocalization with the lysosomal protein LAMP2 as indicated by the Pearson correlation coefficient especially in the perinuclear zone, while in the cellular periphery other vesicles were only positive for LAMP3-GFP or LAMP2 (bar = 10 μm). Quantification was done on three independent slides with 5 fields of view/slide. (B) HeLa cells were transfected with LAMP3-GFP. After 24 h protein was collected in deglycosylation lysis buffer and enzymatically N- and O-deglycosylated. Both glycosylated and deglycosylated samples were analyzed by western blot using an antibody against GFP. Two LAMP3-GFP bands were detected (~90 and ~130 kDa), indicating two different degrees of posttranslational modification. Deglycosylation of LAMP3-GFP resulted in a shift of the two original bands, one of which appeared at the predicted molecular weight of ~70 kDa corresponding to the primary structure of the fusion protein. Another band was detected at ~110 kDa, suggesting the presence of a posttranslational modification resistant to glycosylation. * indicates non-specific band.

after proteasomal inhibition was rather unusual, because MG132 treatment commonly resulted in downregulation or had no effect on PD-associated genes (Fig. S-2). Thus, our data suggest that *LAMP3* participates in the stress response to proteasomal inhibition.

In order to determine if these results obtained with a neuroblastoma cell line could be replicated *in vivo*, mouse brains were infused with the proteasome inhibitor epoxomicin for 24 h or 2 weeks, and the expression of *Lamp3* was measured. The inhibitory effect of epoxomicin at 24 h is evidenced by the upregulation of *Sqstm1* (sequestosome 1, synonymous to p62) to 1.3-fold (Fig. S-3), while the effect of epoxomicin at 2 weeks was previously documented as a ~60% loss of tyrosine-hydroxylase-positive neurons in the midbrain compared to vehicle-infused animals (Subramaniam et al., 2014). As shown in Table 1, *Lamp3* expression was undetectable after 24 h and 2 weeks of treatment, suggesting that additional factors as *e.g.* tumorigenic transformation are needed to induce *Lamp3* expression in the brain.

Autophagic and proteasomal activity differentially regulate the expression of LAMP1, LAMP2, and LAMP3

The next question was if other members of the LAMP family are equally affected by proteasomal inhibition or autophagy induction. Therefore, the expression of *LAMP1*, *LAMP2* and *LAMP3* was measured after starvation or proteasomal inhibition. Incubation of SH-SY5Y cells in HBSS medium for 24 h had no effect on *LAMP1* expression, resulted in upregulation of *LAMP2* (1.6-fold), and caused downregulation of *LAMP3* (0.36-fold) (Fig. 2B). The concentration of the proteasomal inhibitor MG132 was lowered from now on to 300 nM for 24 h, as opposed to 3 μM during 16 h in Fig. 2A, to diminish cell death. Proteasomal inhibition had no effect on *LAMP1* or *LAMP2*, and induced a strong upregulation of *LAMP3* (10.3-fold) (Fig. 2C). Importantly, the strong effect of proteasomal inhibition on *LAMP3* expression could be reproduced in an additional cell line: proteasomal inhibition in HeLa cells resulted also in upregulation

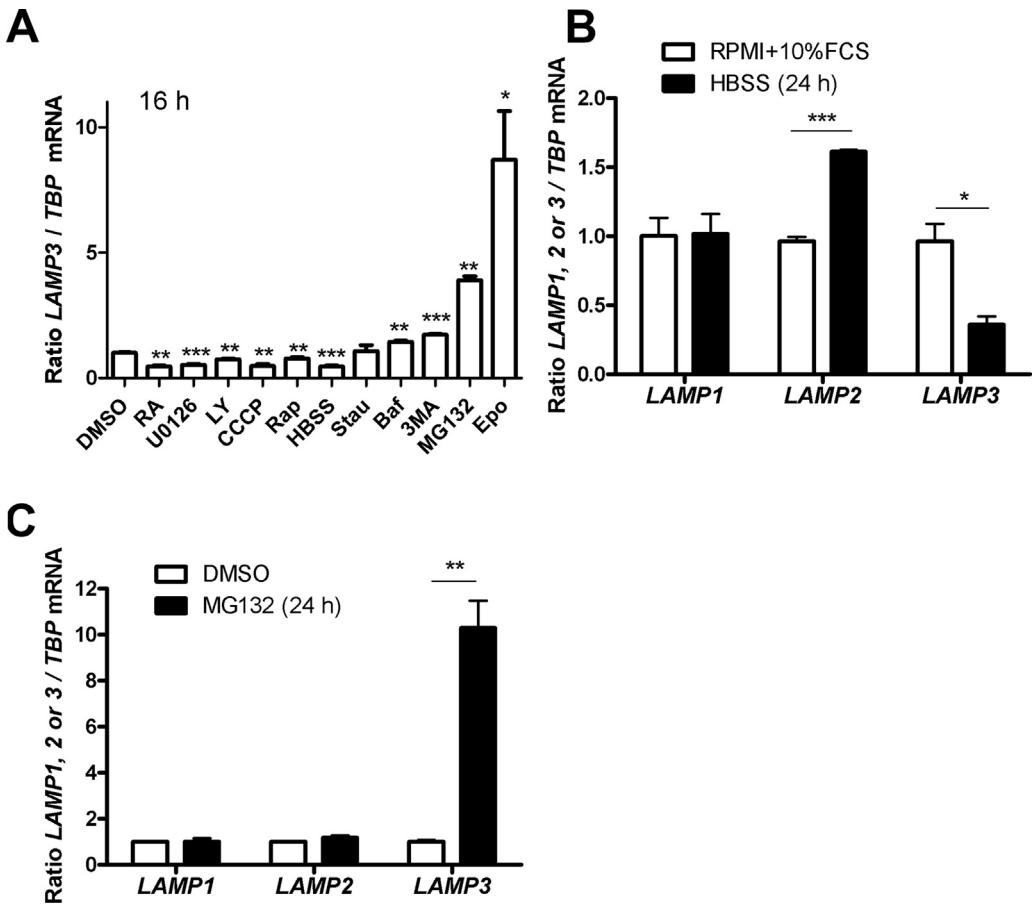

Fig. 2. LAMP3 mRNA levels were modulated by starvation-induced autophagy and proteasomal inhibition. (A) Relative levels of *LAMP3* mRNA were determined by qRT-PCR in SH-SY5Y cells under different conditions. Cellular differentiation was induced with 10 μM retinoic acid (RA) and 3% FCS for 10 days. The following treatments had a duration of 16 h: control medium with 0.05% DMSO, 10 μM U0126, 25 μM LY294002 (LY), 10 nM CCCP, 0.5 μM rapamycin (Rap), starvation medium (HBSS), 30 nM staurosporine (Stau), 10 nM bafilomycin A (Baf), 10 mM 3-methyladenine (3MA), 3 μM MG132, and 1 μM epoxomicin (Epo). *LAMP3* was downregulated by RA-induced differentiation, U0126, LY294002, CCCP, rapamycin- and starvation-induced autophagy. Staurosporine did not affect *LAMP3*. Autophagy inhibition with bafilomycin A1 or 3-methyladenine, and proteasome inhibition with MG132 or epoxomicin induced *LAMP3* upregulation ($n = 3$). (B) SH-SY5Y cells were cultured in complete (RPMI + 10%FCS) or in starvation medium (HBSS) for 24 h. Relative mRNA levels of *LAMP1*, *LAMP2*, and *LAMP3* were determined by qRT-PCR. *LAMP1* mRNA levels remained unchanged, *LAMP2* mRNA levels were significantly upregulated, and *LAMP3* mRNA levels were significantly downregulated by starvation compared to the control ($n = 3$). (C) SH-SY5Y cells were cultured in the presence of 300 nM MG132 or the equivalent concentration of the vehicle (DMSO) for 24 h. Relative mRNA levels of *LAMP1*, *LAMP2*, and *LAMP3* were determined by qRT-PCR. *LAMP1* and *LAMP2* mRNA levels remained unchanged, and *LAMP3* mRNA was robustly induced by proteasomal inhibition compared to the vehicle-treated control ($n = 4$–7). Statistically significant values of t-tests are indicated by $^{*}p \leq 0.05$, $^{**}p \leq 0.01$, and $^{***}p \leq 0.001$.

of *LAMP3* (3.6-fold), but not of *LAMP1* (0.7-fold) or of *LAMP2* (0.6-fold) (Fig. S-4). These results imply that in response to proteasomal dysfunction *LAMP3* is specifically upregulated.

Next, protein expression of LAMP3 was analyzed. The LAMP3 AF4087 antibody recognized bands of the expected size in the positive controls (human lung tissue and HeLa cells overexpressing LAMP3-GFP), but both in SH-SY5Y and HeLa cells a strong non-specific signal covered the region of the endogenous LAMP3 band (Fig. S-5A). Usage of other commercial antibodies (Fig. S-5B and C) or custom-generated *LAMP3* antibodies resulted in nonspecific signals. Thus, it was not possible to confirm the transcriptional data at the protein level.

LAMP3 induction during proteasomal inhibition depends on the ATF4 transcription factor

Previous data showed that *LAMP3* induction by different stressors is depending on the UPR transcription factor ATF4 (Mujcic et al., 2009; Nagelkerke et al., 2013a,b). To determine whether the ATF4 transcription factor controls the expression of LAMP3 during proteasomal stress, the expression of molecules involved in UPR and LAMP genes was measured in cells with and without ATF4 knockdown. SH-SY5Y cells were transfected with *ATF4* siRNA or control siRNA and then exposed to MG132 or DMSO as control for 24 h. Quantitative RT-PCR analyses showed that MG132 treatment induced the expression of *ATF4* (2.1-fold), *LAMP3* (10-fold), as well as the UPR genes *HSPA5* (4.6-fold), and *ATF3* (33-fold) (Fig. 3A). The ~80% reduction of *ATF4* in MG132-treated cells correlated with a reduction of *LAMP3*, *HSPA5*, and *ATF3* expression by 90%, 40%, and 60%, respectively. In contrast, *LAMP1* expression was not affected by ATF4 knockdown, and although *LAMP2* was not induced by MG132 alone, its expression was partially inhibited by *ATF4* siRNA (~0.6-fold) (Fig. 3B). These data indicate that during proteasomal stress *LAMP3* is induced as part of the UPR in an *ATF4*-dependent pathway.

In the reverse experiment the possibility that the knockdown of *LAMP3* exacerbates the UPR and feeds-back onto UPR gene regulation was investigated. To this end, SH-SY5Y cells were transfected with control (CTRL siRNA) or *LAMP3*-targeted siRNA (*LAMP3* siRNA) before initiating MG132 treatment. Afterwards, gene expression of the UPR genes *HSPA5*, *DDIT3*, *ATF3* and *ATF4* was determined by qRT-PCR. Basal levels of *LAMP3* were reduced by 50%, and in the presence of MG132 the 10-fold upregulation was blunted to 2.3-fold (Fig. 4A). Only in the case of *HSPA5* the silencing of *LAMP3* resulted in further upregulation of the corresponding transcript, thus showing that lack of LAMP3 is not enough to exacerbate generalized UPR gene expression (Fig. 4B). In contrast to the MG132-induced

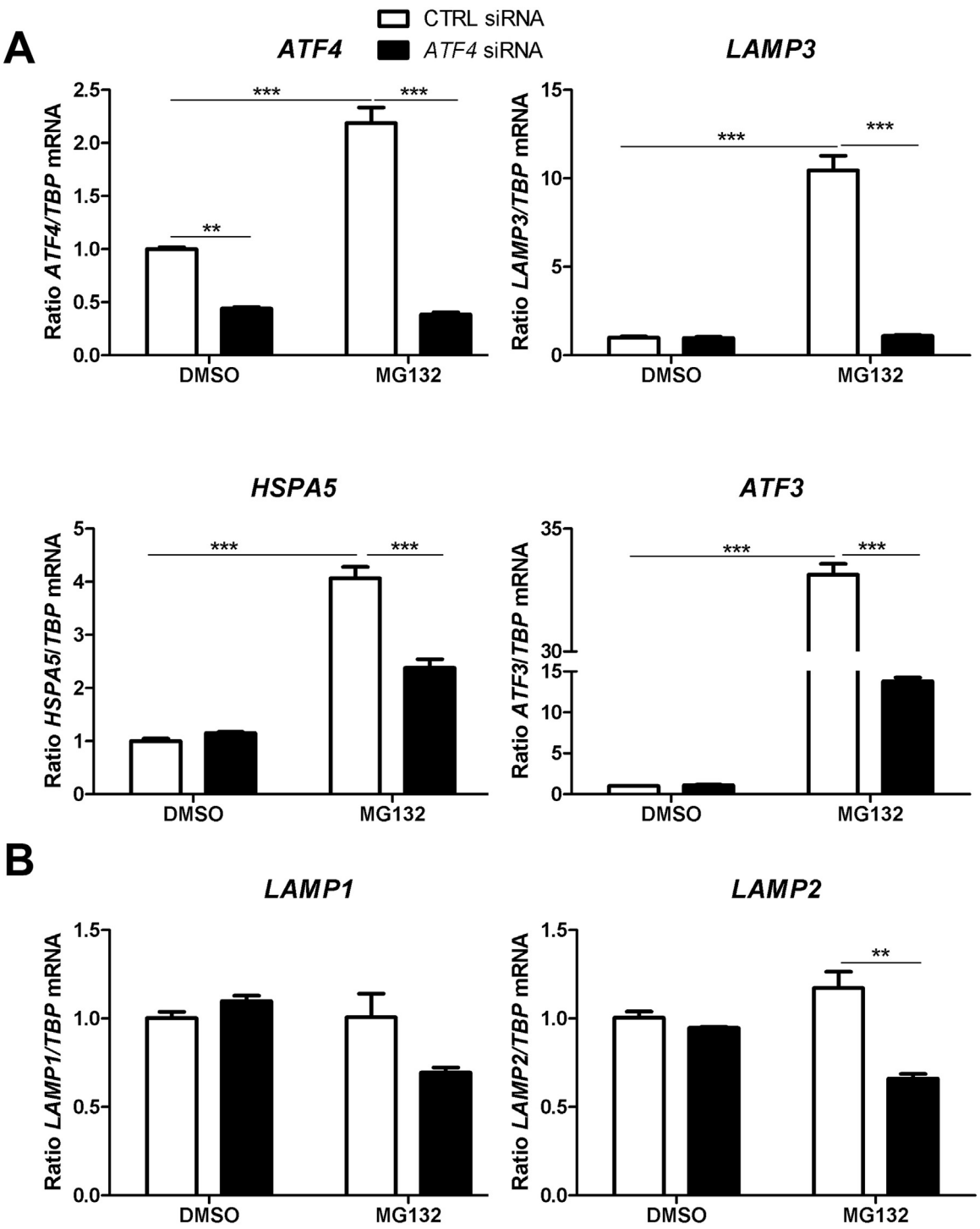

Fig. 3. LAMP3 induction during proteasomal inhibition depends on the transcription factor ATF4. (A) SH-SY5Y cells were transfected either with control siRNA (CTRL siRNA) or with *ATF4*-directed siRNA (*ATF4* siRNA) and after 1 d treated for 24 h with 300 nM MG132 or vehicle. Transcript levels of *ATF4*, *LAMP3*, *HSPA5*, and *ATF3* were determined by qRT-PCR. *ATF4* was induced by MG132 and its induction was inhibited with ~80% efficiency in *ATF4* siRNA transfected samples. ATF4 knockdown prevented the induction of *LAMP3*, and the *UPR* genes *HSPA5* and *ATF3* ($n = 3$). (B) Using the same experimental set-up as in (A), transcript levels of *LAMP1* and *LAMP2* were measured. *LAMP1* was not affected by *ATF4* knockdown. *LAMP2* was not induced due to proteasomal inhibition, but its expression was inhibited by *ATF4* siRNA during MG132 treatment ($n = 3$). Statistical analysis was performed by ANOVA with Bonferroni's *post hoc* test $^{*}p \leq 0.05$, $^{**}p \leq 0.01$, and $^{***}p \leq 0.001$.

upregulation of the UPR genes, analysis of lysosomal and autophagic genes showed either downregulation or no effect in response to MG132 treatment, and this was independent of *LAMP3* (Table S2).

To substantiate our hypothesis that the UPR is involved in the induction of *LAMP3*, SH-SY5Y cells were incubated with thapsigargin or tunicamycin, known ER stressors and activators of the UPR. Both thapsigargin and tunicamycin treatment resulted indeed in a significant upregulation of *LAMP3* and the UPR molecule *HSPA5*, but not *LAMP1* or *LAMP2* (Fig. S-6). Taken together, these findings support the notion that *LAMP3* is induced as part of the UPR in SH-SY5Y cells during proteasomal inhibition.

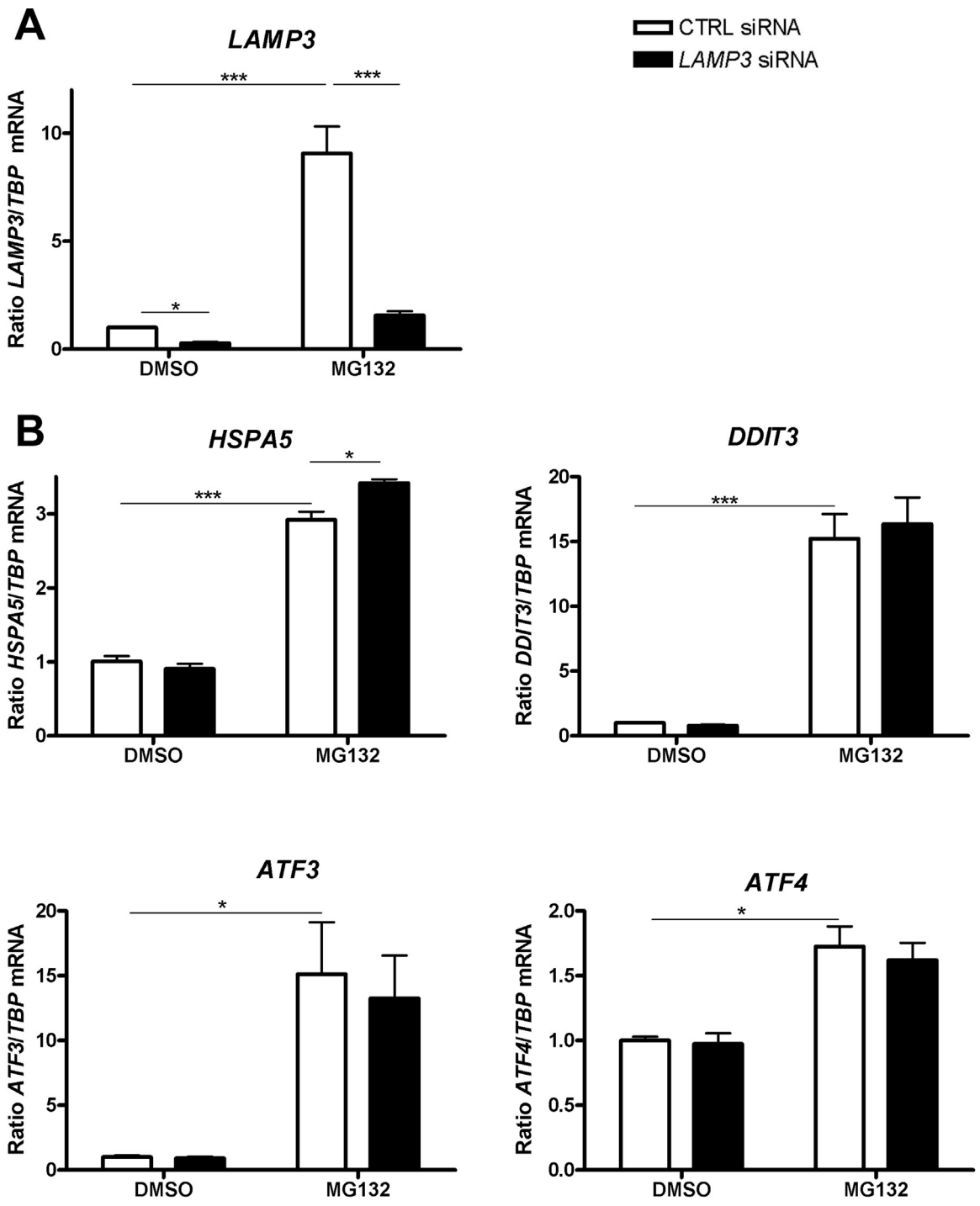

Fig. 4. LAMP3 regulates HSPA5 gene expression during proteasomal inhibition. (A) SH-SY5Y cells were transfected with control siRNA (CTRL siRNA) or with *LAMP3*-targeted siRNA (*LAMP3* siRNA) and after 1 d cells were treated for 24 h with 300 nM MG132 or equivalent concentration of the vehicle DMSO. Relative levels of *LAMP3* were determined by qRT-PCR. Basal *LAMP3* levels and *LAMP3* upregulation induced by MG132 were significantly reduced by *LAMP3* siRNA treatment ($n = 8$). (B) Using the same experimental set-up as in (A), relative mRNA levels of *HSPA5*, *DDIT3*, *ATF3*, and *ATF4* were determined by qRT-PCR in SH-SY5Y cells. MG132-mediated proteasomal inhibition resulted in upregulation of *HSPA5*, *DDIT3*, *ATF3*, and *ATF4*. Prevention of *LAMP3* upregulation resulted in an increase of *HSPA5*, but had no effect on the other genes ($n = 3$). Statistical analysis was performed by ANOVA with Bonferroni's *post hoc* test $^{*}p \leq 0.05$, $^{**}p \leq 0.01$, and $^{***}p \leq 0.001$.

LAMP3 upregulation is contributing to autophagic flux induction after proteasomal inhibition

Proteasomal dysfunction prompts compensatory autophagy (Korolchuk et al., 2010; Nedelsky et al., 2008; Park and Cuervo, 2013), the unfolded protein response (UPR) being one of the proposed crosstalk pathways between these two systems (Korolchuk et al., 2010). Therefore, the influence of *LAMP3* on autophagy during proteasomal inhibition was assessed by measuring SQSTM1/p62 at the transcript and protein level, as well as the formation of LC3-II as parameters for autophagy and autophagic flux (Mizushima et al., 2010). SQSTM1was determined in SH-SY5Y cells with and without *LAMP3* knockdown and MG132 exposure. Measurement of *SQSTM1* mRNA showed an 11-fold induction upon MG132 treatment, and this induction was not affected by knockdown of *LAMP3* (Fig. 5A). At the protein level, SQSTM1 was expressed only minimally in

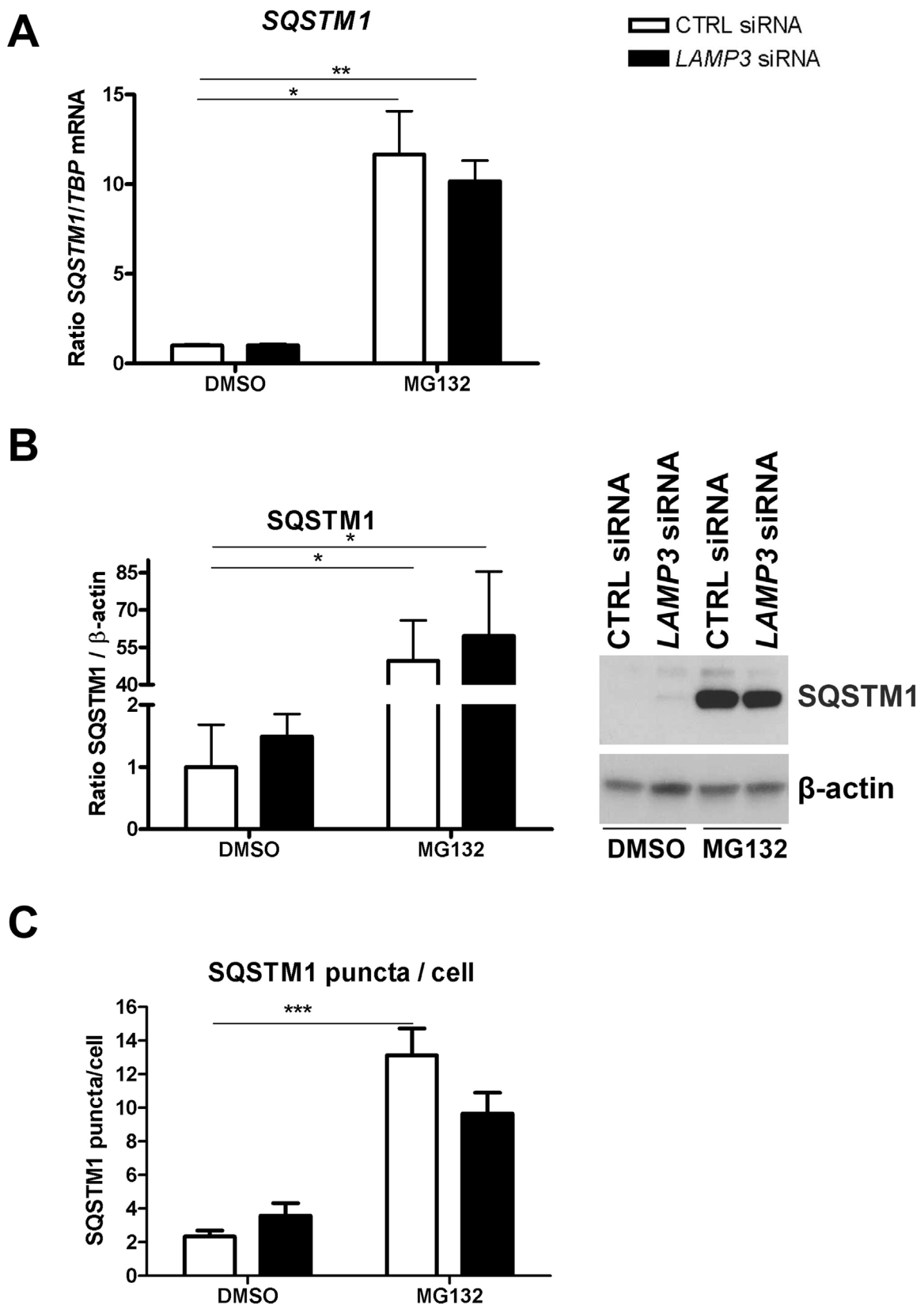

Fig. 5. SQSTM1 induction and puncta formation is independent of LAMP3. (A) SH-SY5Y cells were transfected with CTRL siRNA or *LAMP3* siRNA and after 1 d exposed to 300 nM MG132 or DMSO for 24 h. *SQSTM1* was measured by qRT-PCR. Proteasomal inhibition with MG132 resulted in upregulation of *SQSTM1* ($n = 3$). (B) Cells were transfected and treated with MG132 as in (A) and total protein was analyzed by western blot using an antibody against SQSTM1. A representative western blot as well as the densitometric analysis is shown. SQSTM1 was strongly induced by MG132 treatment, and the extent of its induction was not affected by silencing of *LAMP3* ($n = 3$). (C) Cells were transfected and treated with MG132 as in (A), and stained with an antibody against SQSTM1. The number of SQSTM1 puncta per cell was determined by confocal microscopy. The number of puncta per cell was increased by MG132 treatment, independently of *LAMP3* induction. A total of 20–70 cells in at least 5 randomly chosen fields of view were used in the quantification. A representative image is shown in Fig. S-7A. Statistical analysis was performed by ANOVA with Bonferroni's *post hoc* test $^{*}p \leq 0.05$, $^{**}p \leq 0.01$, and $^{***}p \leq 0.001$.

control conditions; upon MG132 treatment its expression increased strongly (~50-fold) and was not influenced by the silencing of *LAMP3* (Fig. 5B). Treatment with MG132 increased the number of SQSTM1 signals (puncta), which are most probably associated with LC3-positive autophagosomes (Sahani et al., 2014). However, their number was not affected by the knockdown of *LAMP3* (Fig. 5C and Fig. S-7A).

Another crucial marker to monitor autophagy is the assessment of LC3-I conversion to LC3-II in the presence and absence of inhibitors of autophagosome-lysosome fusion, as bafilomycin A1 (Mizushima et al., 2010). We showed before that in SH-SY5Y cells a LC3-II band in the absence of bafilomycin A1 is not detectable even in cells starved for more than 12 h (Klinkenberg et al., 2012), probably due to strong autophagic flux. Therefore, analysis of LC3-II in SH-SY5Y cells was monitored only in the presence of bafilomycin A1. As predicted, proteasomal inhibition resulted in an upregulation of autophagic flux (ratio LC3-II/GAPDH) (3.1-fold). Importantly, siRNA-mediated *LAMP3* silencing resulted in an impaired induction of autophagic flux (1.9-fold) (Fig. 6A), indicating that *LAMP3* is necessary for the induction of autophagy upon proteasomal dysfunction despite unchanged SQSTM1 levels (see Discussion).

As LAMP3 is a lysosomal protein, potential changes in lysosome number and distribution after *LAMP3* knockdown were assessed. Cells were transfected with *LAMP3* siRNA or control siRNA, treated with MG132 or DMSO, and immunostained for the lysosomal marker LAMP1. No significant changes were observed in the distribution or the amount of LAMP1-positive vesicles per cell (Fig. 6B and Fig. S-7B). This suggests that the alteration in autophagic flux during MG132 treatment is not mediated by changes in lysosomal number.

To determine whether the effect of *LAMP3* siRNA on autophagic flux is specific for proteasomal inhibition, the influence of *LAMP3* on starvation-induced autophagy was measured. Fig. 6C shows that the autophagic flux in cells cultured in starvation medium was not affected by the knockdown of *LAMP3*. This indicates that *LAMP3* specifically influences autophagic flux induced by proteasomal inhibition, but not by starvation.

LAMP3 is necessary for cell survival during proteasomal inhibition

As shown above and detailed in the discussion, autophagy induction is a fundamental cellular survival response to proteasomal dysfunction. Given that autophagy induction as a result of proteasomal inhibition was impaired in LAMP3-silenced cells, the role of LAMP3 in cell survival was evaluated. SH-SY5Y cells were transiently transfected with the *LAMP3*-targeted siRNA or a control siRNA, and either treated with MG132 or DMSO. After 24 h apoptosis was quantified by two methods that determine caspase-3 activation. Proteasomal inhibition resulted in a strong induction of apoptosis measured by caspase-3 activity (13.5-fold), which was further increased in cells that were previously transfected with the siRNA targeting *LAMP3* (17.8-fold) (Fig. 7A). This result could be confirmed by measuring the cleavage of PARP, an early substrate of caspase-3. Proteasomal inhibition resulted in increased appearance of the 89 kDa PARP fragment, and the prevention of *LAMP3* upregulation resulted in a further increase of PARP cleavage (Fig. 7B). A rescue experiment by transfecting SH-SY5Y cells with LAMP3-GFP prior to MG132 treatment was not successful, due to the low transfection efficiency of LAMP3-GFP in this cell line.

To determine whether the effect of LAMP3 knockdown on apoptosis is specific for proteasomal inhibition, cells were transfected with *LAMP3* siRNA and treated for 6 h with the kinase inhibitor staurosporine, a well-known inducer of apoptosis. As shown in Fig. 7C, exposure to staurosporine resulted in a strong increase of caspase-3 activity, which was however not influenced by *LAMP3*. These data point to a specific function of *LAMP3* in proteasomal inhibition.

In summary, our data show that upregulation of *LAMP3* in SH-SY5Y cells is necessary for the response to proteasomal inhibition in order to promote cell survival.

Discussion

Recent genome-wide association studies of PD have identified variants at the locus *MCCC1/LAMP3* as risk factors, although *LAMP3* was not detected in brain tissue (Akasaki et al., 2004; de Saint-Vis et al., 1998; Kanao et al., 2005; Salaun et al., 2004). With this finding as starting point we investigated a possible function that LAMP3 could have in the progression of PD. Neither overexpression of the mutant human A53T-α-synuclein nor the infusion of a proteasomal inhibitor induced the expression of *LAMP3* in mouse brain. Furthermore, LAMP3 mRNA and protein was not detected in the posterior cingulate gyrus of PD cases and age-/gender-matched controls. Recently, Murphy and colleagues reported that early and late cases of PD as well as age-matched controls expressed LAMP3 protein in the anterior cingulate and that there were no significant differences between these two groups (Murphy et al., 2014). In our hands, the same antibody also detected a band at ~65 kDa in HeLa cells. But this signal was not affected by *LAMP3* siRNA transfection or deglycosylation; thus, we assume that it represents a non-specific band (Fig. S-5B). While the expression of LAMP3 in other brain regions should not be ruled out, our data indicate no direct association of LAMP3 with the neuronal pathomechanisms that are contributing to PD. Further investigation is needed to understand how the *MCCC1/LAMP3* locus contributes to the initiation or progression of PD. Possible mechanisms could include the participation of *LAMP3* in cellular physiology outside the brain, or the involvement of other genes present in the *MCCC1/LAMP3* locus.

In contrast to the absence of *LAMP3* in brain, the cell line SH-SY5Y, originating from a neuroblastoma tumor, expresses this gene. The LAMP3 expression is probably due to the tumorigenic nature of the cell line, as LAMP3 is involved in cellular transformation and invasiveness in cervical, breast, and prostate cancer cells (Kanao et al., 2005; Nagelkerke et al., 2011; Pennati et al., 2013). In support of this hypothesis, differentiation of SH-SH5Y cells with retinoic acid reduced *LAMP3* levels by 50%.

Using different pharmacologic modulators, proteasomal inhibitors were identified as strong inducers of *LAMP3* expression. Previous reports have shown that the LAMP3 expression is ATF4-dependent during hypoxia (Nagelkerke et al., 2013a,b). Our results imply that the mechanism that controls *LAMP3* expression during proteasomal stress is the UPR because (1) knockdown of the UPR transcription factor ATF4 prevented the induction of *LAMP3* by MG132 treatment, (2) other molecules of the UPR were induced similar to *LAMP3*, and (3) direct activation of the UPR with thapsigargin or tunicamycin strongly triggered *LAMP3*, but not *LAMP1* or *LAMP2* induction. Thus, our data indicate that proteasomal inhibition activates *LAMP3* expression *via* the UPR in neuroblastoma cells. Despite a lot of effort dedicated to this subject, the induction of LAMP3 at the protein level could not be determined due to crossreactivity or nonspecificity of several commercial LAMP3 antibodies.

Consistent with other reports (Lan et al., 2015; Tang et al., 2014), analysis of the autophagosome marker LC3-II showed that proteasomal inhibition promoted enhancement of the autophagic flux. Silencing of LAMP3 impaired the induction of autophagic flux and promoted cell death. As indicator of autophagic flux we relied on the autophagosomal marker LC3-II rather than SQSTM1/p62. SQSTM1 interacts on the one hand with the ubiquitin moiety in ubiquitin-tagged protein substrates, and on the other hand with LC3-II for subsequent autophagic degradation (Lamark et al., 2009). As can be seen in Fig. 5B and C, the basal levels of SQSTM1 protein

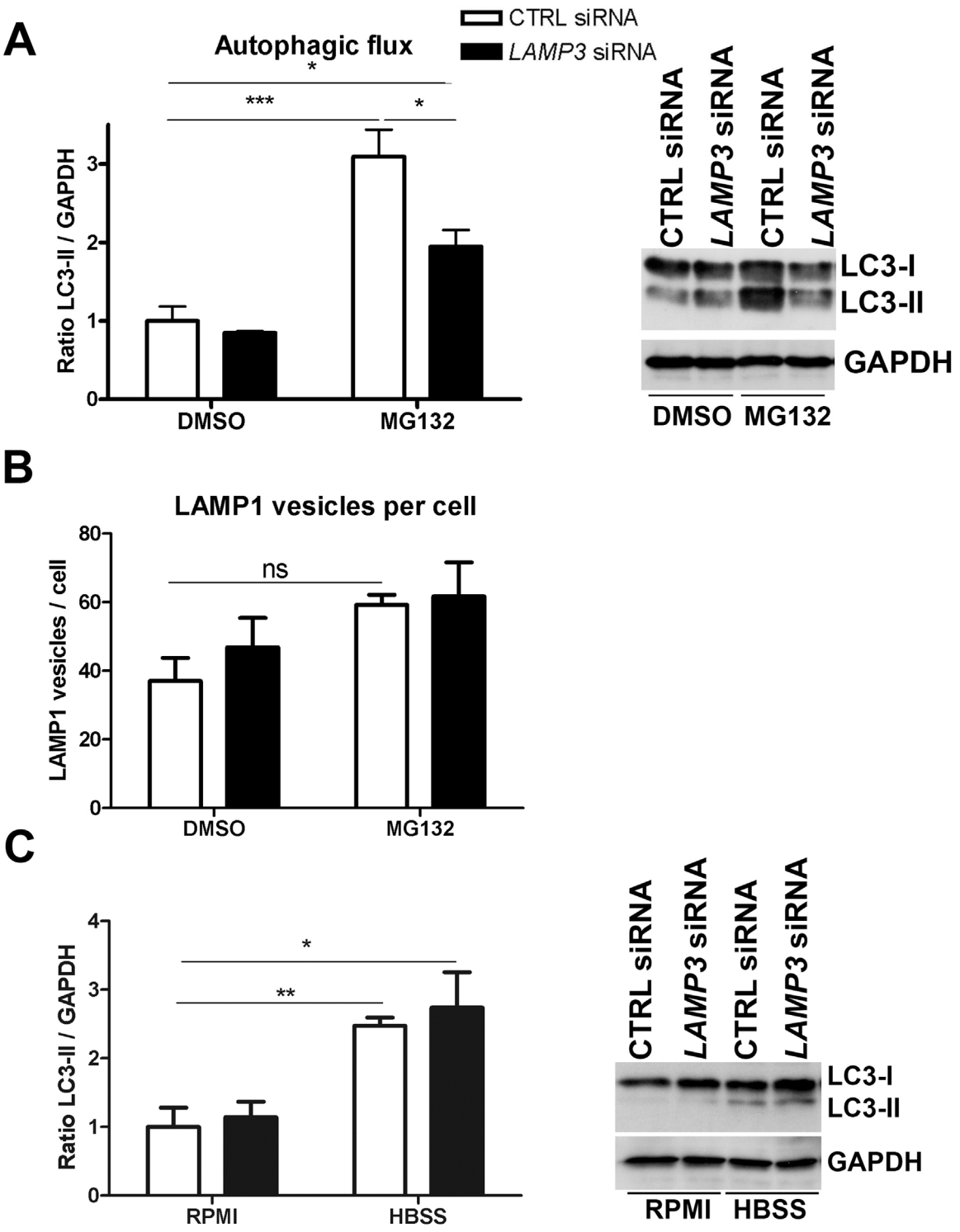

Fig. 6. Prevention of LAMP3 mRNA upregulation resulted in impaired autophagic flux during proteasomal inhibition. (A) Autophagic flux was analyzed in SH-SY5Y cells with or without *LAMP3* knockdown either in control conditions (DMSO) or in the presence of 300 nM MG132 for 24 h. Bafilomycin A1 was added at a final concentration of 10 nM during the last 2 h of culture. Total protein was analyzed by western blot using an anti-LC3 antibody, and GAPDH as loading control. A representative western blot as well as the densitometric analysis is shown. Autophagic flux was impaired by *LAMP3* siRNA in MG132-treated cells ($n = 3$). (B) The number of LAMP1-positive vesicles per cell was quantified in cells with or without *LAMP3* knockdown and treated with MG132 or DMSO. Cells were fixed, stained with an antibody against LAMP1, and analyzed by confocal microscopy. The number of LAMP1-positive vesicles was not affected by MG132 treatment or *LAMP3* knockdown. A total of 20–70 cells in at least 5 randomly chosen fields of view were used for the quantification. A representative image is shown in Fig. S-7B. (C) Autophagic flux was analyzed in SH-SY5Y cells with or without *LAMP3* knockdown either in control conditions (RPMI) or in starvation medium (HBSS) for 2 h. In all cases 10 nM bafilomycin A1 was present in the culture. Total protein was analyzed by western blot using an anti-LC3 antibody, and GAPDH as loading control. A representative western blot as well as the densitometric analysis is shown. Autophagic flux was not influenced by *LAMP3* siRNA in starved cells ($n = 4$). Statistical analysis was performed by ANOVA with Bonferroni's *post hoc* test $^{*}p \leq 0.05$, $^{**}p \leq 0.01$, and $^{***}p \leq 0.001$.

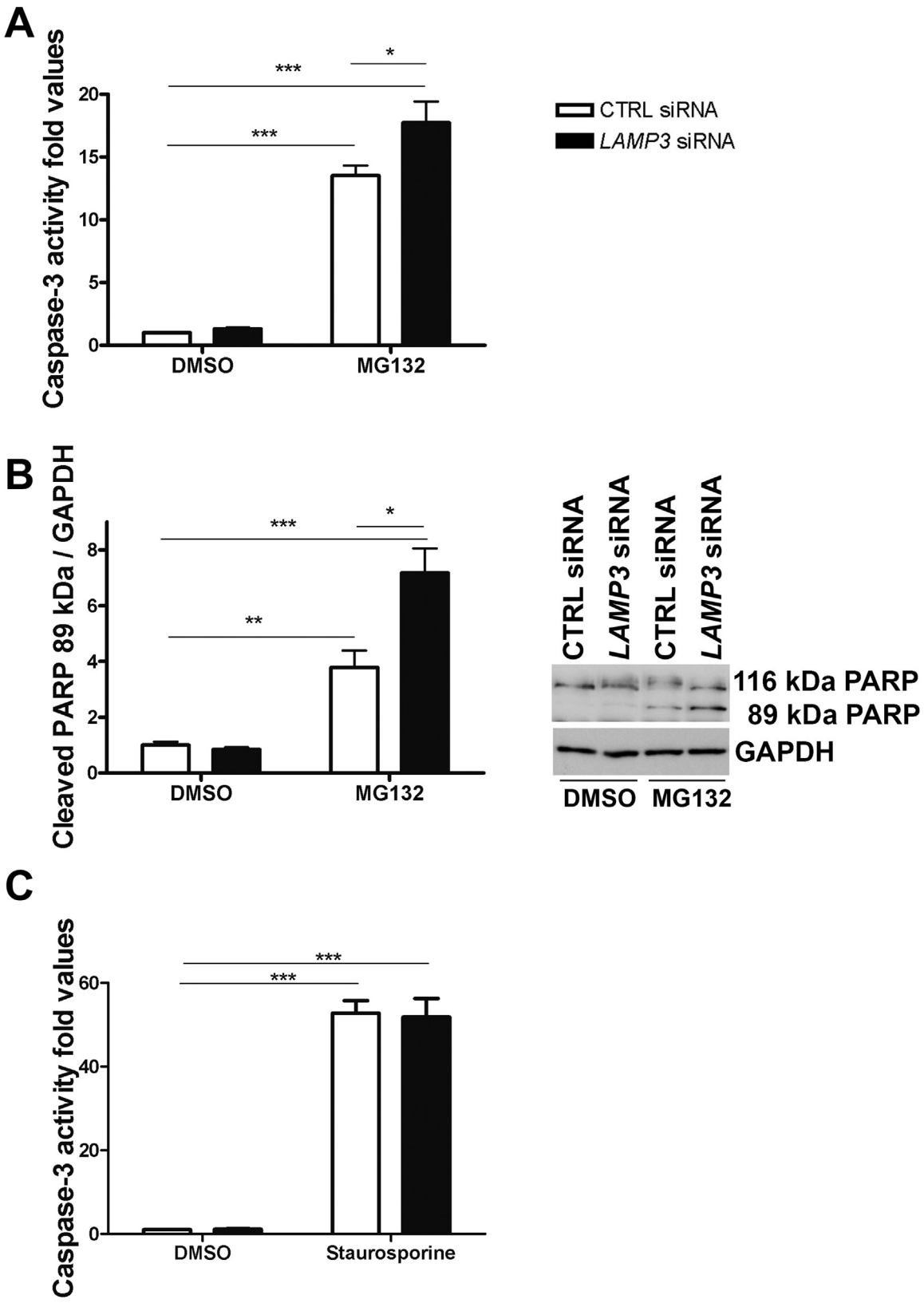

Fig. 7. Prevention of LAMP3 mRNA upregulation resulted in increased apoptosis during proteasomal inhibition. (A) SH-SY5Y cells were transfected with CTRL siRNA or *LAMP3* siRNA and after 1 d exposed to 300 nM MG132 or DMSO for 24 h. Caspase-3 activity analysis was performed as indicated in materials and methods. Knockdown of *LAMP3* resulted in an increase of MG132-induced caspase-3 activity. Results were normalized to protein amount and shown relative to DMSO + CTRL siRNA ($n = 5$). (B) SH-SY5Y cells were transfected with CTRL siRNA or *LAMP3* siRNA, cultured overnight and then exposed to 300 nM MG132 or DMSO for 24 h. Cleavage of Poly-ADP Ribose Polymerase (PARP) was determined by western blot. Increased cleaved PARP 89 kDa was observed upon proteasomal inhibition, and a further increase was observed in *LAMP3* siRNA-transfected cells ($n = 4$). (C) SH-SY5Y cells were transfected with CTRL siRNA or *LAMP3* siRNA and after 1 d exposed to 30 nM staurosporine or DMSO for 6 h. Caspase-3 activity analysis was performed as indicated in materials and methods. Knockdown of *LAMP3* did not affect caspase-3 activity induced by staurosporine. Results were normalized to protein amount and shown relative to DMSO + CTRL siRNA ($n = 3$–5). Statistical analysis was performed by ANOVA with Bonferroni's *post hoc* test $^{*}p \leq 0.05$, $^{**}p \leq 0.01$, and $^{***}p \leq 0.001$.

were very low and increased strongly after MG132-triggered proteasomal inhibition. It seems likely that an additional effect due to *LAMP3* silencing would not be detectable in this strong reaction.

The mechanism that mediates the induction of autophagic flux following proteasome inhibition seems to depend on the UPR. In support of this hypothesis, it was reported that the transcription factor ATF4 mediates autophagy in response to the proteasome inhibitors bortezomib and oprozomib in multiple myeloma and other cancers (Rzymski et al., 2009; Zang et al., 2012). Therefore, we propose the following scenario in our model: proteasomal inhibition with MG132 activates the ATF4 pathway of the UPR, thus driving LAMP3 expression and promoting autophagic flux. During proteasomal inhibition enhancement of the autophagic pathway acts as compensatory response to degrade accumulated proteasome substrates. It is important to stress MG132-mediated ATF4 signaling pathway is primarily targeting LAMP3 and not LAMP1, and only slightly influencing LAMP2. Given that LAMP3 and LAMP2 signals did not entirely colocalize in immunofluorescence and that the number, appearance and distribution of lysosomes and p62-positive puncta/autophagosomes did not change after LAMP3 knockdown, it is tempting to speculate that LAMP3 has a role in autophagosome maturation and/or autophagosome-lysosome fusion.

In case of *LAMP3* deficiency, autophagy induction is impaired, and the autophagy-lysosomal pathway is overtaxed resulting in further accumulation of non-degraded substrates. With both of the major degradation pathways dysfunctional, apoptosis is enhanced.

This hypothesis is supported by previous studies revealing the participation of *LAMP3* in autophagy and cellular viability in different cancer cells. One report showed that breast cancer cells resistant to the cytostatic drug tamoxifen expressed 7-times more *LAMP3* mRNA than sensitive cells, and exhibited significantly higher autophagic activity. Importantly, siRNA-mediated *LAMP3* silencing resulted in autophagy inhibition and restored tamoxifen sensitivity (Nagelkerke et al., 2014). Furthermore, prostate cancer cells resistant to the chemotherapeutic cisplatin can be resensitized to the drug by the knockdown of *LAMP3*. This effect seems mediated by the impairment of autophagic flux (Pennati et al., 2013).

As recent data indicate that autophagy and the ubiquitin-proteasome system have crucial roles for tumor development and metastasis (Errafiy et al., 2013; Qiang et al., 2014; Vogl et al., 2014), our findings that *LAMP3* participates in the response to proteasomal dysfunction are relevant for cancer research. The proteasomal inhibitor bortezomib is approved for the treatment of multiple myeloma, but its effectiveness is limited against breast tumors (Combaret et al., 2008; Mujtaba and Dou, 2011). In addition, cancer cells often develop resistance to chemotherapy (Furfaro et al., 2014) and the resistance mechanisms include the induction of the UPR and autophagy (Milani et al., 2009). Accordingly, *LAMP3* could be involved in the development of resistance to proteasomal inhibitors during chemotherapy.

In conclusion, we report a previously unknown transcriptional upregulation of LAMP3 expression after proteasomal stress, which is contributing to promote autophagy and cell survival.

Acknowledgements

Brain tissue was obtained from the Neurobiobank Munich/Brain-Net Germany (http://www.brain-net.net), and we are grateful to Dr. Thomas Arzberger and colleagues for it. We thank Prof. Deller, Dr. Domenico del Turco and Heike Korff for the RNA integrity analysis of human brain tissues. We are grateful to Birgitt Meseck-Selchow for technical assistance. The study was financially supported by the NGFNplus Parkinson network (BMBF 01GS08138), by the ERANET-NEURON-RePARK 2009 network (BMBF 01EW1012), and by the GerontoMitoSys network (BMBF 0315584A).

Appendix A. Supplementary data

Supplementary data associated with this article can be found, in the online version, at http://dx.doi.org/10.1016/j.ejcb.2015.01.003.

References

Akasaki, K., Nakamura, N., Tsukui, N., Yokota, S., Murata, S., Katoh, R., Michihara, A., Tsuji, H., Marques Jr., E.T., August, J.T., 2004. Human dendritic cell lysosome-associated membrane protein expressed in lung type II pneumocytes. Arch. Biochem. Biophys. 425, 147–157.

Andrejewski, N., Punnonen, E.L., Guhde, G., Tanaka, Y., Lullmann-Rauch, R., Hartmann, D., von Figura, K., Saftig, P., 1999. Normal lysosomal morphology and function in LAMP-1-deficient mice. J. Biol. Chem. 274, 12692–12701.

Braak, H., Braak, E., 1991. Neuropathological stageing of Alzheimer-related changes. Acta Neuropathol. 82, 239–259.

Braak, H., Del Tredici, K., Rub, U., de Vos, R.A., Jansen Steur, E.N., Braak, E., 2003. Staging of brain pathology related to sporadic Parkinson's disease. Neurobiol. Aging 24, 197–211.

Combaret, V., Boyault, S., Iacono, I., Brejon, S., Rousseau, R., Puisieux, A., 2008. Effect of bortezomib on human neuroblastoma: analysis of molecular mechanisms involved in cytotoxicity. Mol. Cancer 7, 50.

de Saint-Vis, B., Vincent, J., Vandenabeele, S., Vanbervliet, B., Pin, J.J., Ait-Yahia, S., Patel, S., Mattei, M.G., Banchereau, J., Zurawski, S., Davoust, J., Caux, C., Lebecque, S., 1998. A novel lysosome-associated membrane glycoprotein, DC-LAMP, induced upon DC maturation, is transiently expressed in MHC class II compartment. Immunity 9, 325–336.

Errafiy, R., Aguado, C., Ghislat, G., Esteve, J.M., Gil, A., Loutfi, M., Knecht, E., 2013. PTEN increases autophagy and inhibits the ubiquitin-proteasome pathway in glioma cells independently of its lipid phosphatase activity. PLOS ONE 8, e83318.

Eskelinen, E.L., Schmidt, C.K., Neu, S., Willenborg, M., Fuertes, G., Salvador, N., Tanaka, Y., Lullmann-Rauch, R., Hartmann, D., Heeren, J., von Figura, K., Knecht, E., Saftig, P., 2004. Disturbed cholesterol traffic but normal proteolytic function in LAMP-1/LAMP-2 double-deficient fibroblasts. Mol. Biol. Cell 15, 3132–3145.

Furfaro, A.L., Piras, S., Passalacqua, M., Domenicotti, C., Parodi, A., Fenoglio, D., Pronzato, M.A., Marinari, U.M., Moretta, L., Traverso, N., Nitti, M., 2014. HO-1 up-regulation: a key point in high-risk neuroblastoma resistance to bortezomib. Biochim. Biophys. Acta 1842, 613–622.

Gispert, S., Del Turco, D., Garrett, L., Chen, A., Bernard, D.J., Hamm-Clement, J., Korf, H.W., Deller, T., Braak, H., Auburger, G., Nussbaum, R.L., 2003. Transgenic mice expressing mutant A53T human alpha-synuclein show neuronal dysfunction in the absence of aggregate formation. Mol. Cell. Neurosci. 24, 419–429.

Glickman, M.H., Ciechanover, A., 2002. The ubiquitin-proteasome proteolytic pathway: destruction for the sake of construction. Physiol. Rev. 82, 373–428.

He, C., Klionsky, D.J., 2009. Regulation mechanisms and signaling pathways of autophagy. Annu. Rev. Genet. 43, 67–93.

Kanao, H., Enomoto, T., Kimura, T., Fujita, M., Nakashima, R., Ueda, Y., Ueno, Y., Miyatake, T., Yoshizaki, T., Buzard, G.S., Tanigami, A., Yoshino, K., Murata, Y., 2005. Overexpression of LAMP3/TSC403/DC-LAMP promotes metastasis in uterine cervical cancer. Cancer Res. 65, 8640–8645.

Klinkenberg, M., Gispert, S., Dominguez-Bautista, J.A., Braun, I., Auburger, G., Jendrach, M., 2012. Restriction of trophic factors and nutrients induces PARKIN expression. Neurogenetics 13, 9–21.

Korolchuk, V.I., Menzies, F.M., Rubinsztein, D.C., 2010. Mechanisms of cross-talk between the ubiquitin-proteasome and autophagy-lysosome systems. FEBS Lett. 584, 1393–1398.

Lamark, T., Kirkin, V., Dikic, I., Johansen, T., 2009. NBR1 and p62 as cargo receptors for selective autophagy of ubiquitinated targets. Cell Cycle 8, 1986–1990.

Lan, D., Wang, W., Zhuang, J., Zhao, Z., 2015. Proteasome inhibitor-induced autophagy in PC12 cells overexpressing A53T mutant alpha-synuclein. Mol. Med. Rep. 11, 1655–1660.

Li, N.N., Tan, E.K., Chang, X.L., Mao, X.Y., Zhao, D.M., Zhang, J.H., Liao, Q., Peng, R., 2013. MCCC1/LAMP3 reduces risk of sporadic Parkinson's disease in Han Chinese. Acta Neurol. Scand. 128, 136–139.

Lill, C.M., Roehr, J.T., McQueen, M.B., Kavvoura, F.K., Bagade, S., Schjeide, B.M., Schjeide, L.M., Meissner, E., Zauft, U., Allen, N.C., Liu, T., Schilling, M., Anderson, K.J., Beecham, G., Berg, D., Biernacka, J.M., Brice, A., DeStefano, A.L., Do, C.B., Eriksson, N., Factor, S.A., Farrer, M.J., Foroud, T., Gasser, T., Hamza, T., Hardy, J.A., Heutink, P., Hill-Burns, E.M., Klein, C., Latourelle, J.C., Maraganore, D.M., Martin, E.R., Martinez, M., Myers, R.H., Nalls, M.A., Pankratz, N., Payami, H., Satake, W., Scott, W.K., Sharma, M., Singleton, A.B., Stefansson, K., Toda, T., Tung, J.Y., Vance, J., Wood, N.W., Zabetian, C.P., Young, P., Tanzi, R.E., Khoury, M.J., Zipp, F., Lehrach, H., Ioannidis, J.P., Bertram, L., 2012. Comprehensive research synopsis and systematic meta-analyses in Parkinson's disease genetics: the PDGene database. PLoS Genet. 8, e1002548.

Milani, M., Rzymski, T., Mellor, H.R., Pike, L., Bottini, A., Generali, D., Harris, A.L., 2009. The role of ATF4 stabilization and autophagy in resistance of breast cancer cells treated with Bortezomib. Cancer Res. 69, 4415–4423.

Mizushima, N., 2007. Autophagy: process and function. Genes Dev. 21, 2861–2873.

Mizushima, N., Yoshimori, T., Levine, B., 2010. Methods in mammalian autophagy research. Cell 140, 313–326.
Mujcic, H., Rzymski, T., Rouschop, K.M., Koritzinsky, M., Milani, M., Harris, A.L., Wouters, B.G., 2009. Hypoxic activation of the unfolded protein response (UPR) induces expression of the metastasis-associated gene LAMP3. Radiother. Oncol. 92, 450–459.
Mujtaba, T., Dou, Q.P., 2011. Advances in the understanding of mechanisms and therapeutic use of bortezomib. Discov. Med. 12, 471–480.
Murphy, K.E., Gysbers, A.M., Abbott, S.K., Tayebi, N., Kim, W.S., Sidransky, E., Cooper, A., Garner, B., Halliday, G.M., 2014. Reduced glucocerebrosidase is associated with increased alpha-synuclein in sporadic Parkinson's disease. Brain 137, 834–848.
Nagelkerke, A., Bussink, J., Mujcic, H., Wouters, B.G., Lehmann, S., Sweep, F.C., Span, P.N., 2013a. Hypoxia stimulates migration of breast cancer cells via the PERK/ATF4/LAMP3-arm of the unfolded protein response. Breast Cancer Res. 15, R2.
Nagelkerke, A., Bussink, J., van der Kogel, A.J., Sweep, F.C., Span, P.N., 2013b. The PERK/ATF4/LAMP3-arm of the unfolded protein response affects radioresistance by interfering with the DNA damage response. Radiother. Oncol. 108, 415–421.
Nagelkerke, A., Mujcic, H., Bussink, J., Wouters, B.G., van Laarhoven, H.W., Sweep, F.C., Span, P.N., 2011. Hypoxic regulation and prognostic value of LAMP3 expression in breast cancer. Cancer 117, 3670–3681.
Nagelkerke, A., Sieuwerts, A.M., Bussink, J., Sweep, F.C., Look, M.P., Foekens, J.A., Martens, J.W., Span, P.N., 2014. LAMP3 is involved in tamoxifen resistance in breast cancer cells through the modulation of autophagy. Endocr. Relat. Cancer 21, 101–112.
Nedelsky, N.B., Todd, P.K., Taylor, J.P., 2008. Autophagy and the ubiquitin-proteasome system: collaborators in neuroprotection. Biochim. Biophys. Acta 1782, 691–699.
Ozaki, K., Nagata, M., Suzuki, M., Fujiwara, T., Ueda, K., Miyoshi, Y., Takahashi, E., Nakamura, Y., 1998. Isolation and characterization of a novel human lung-specific gene homologous to lysosomal membrane glycoproteins 1 and 2: significantly increased expression in cancers of various tissues. Cancer Res. 58, 3499–3503.
Parganlija, D., Klinkenberg, M., Dominguez-Bautista, J., Hetzel, M., Gispert, S., Chimi, M.A., Drose, S., Mai, S., Brandt, U., Auburger, G., Jendrach, M., 2014. Loss of PINK1 impairs stress-induced autophagy and cell survival. PLOS ONE 9, e95288.
Park, C., Cuervo, A.M., 2013. Selective autophagy: talking with the UPS. Cell Biochem. Biophys. 67, 3–13.
Pennati, M., Lopergolo, A., Profumo, V., De Cesare, M., Sbarra, S., Valdagni, R., Zaffaroni, N., Gandellini, P., Folini, M., 2013. miR-205 impairs the autophagic flux and enhances cisplatin cytotoxicity in castration-resistant prostate cancer cells. Biochem. Pharmacol.
Pihlstrom, L., Axelsson, G., Bjornara, K.A., Dizdar, N., Fardell, C., Forsgren, L., Holmberg, B., Larsen, J.P., Linder, J., Nissbrandt, H., Tysnes, O.B., Ohman, E., Dietrichs, E., Toft, M., 2013. Supportive evidence for 11 loci from genome-wide association studies in Parkinson's disease. Neurobiol. Aging 34 (170), e1707–e1713.
Qiang, L., Zhao, B., Ming, M., Wang, N., He, T.C., Hwang, S., Thorburn, A., He, Y.Y., 2014. Regulation of cell proliferation and migration by p62 through stabilization of Twist1. Proc. Natl. Acad. Sci. U. S. A. 111, 9241–9246.
Rzymski, T., Milani, M., Singleton, D.C., Harris, A.L., 2009. Role of ATF4 in regulation of autophagy and resistance to drugs and hypoxia. Cell Cycle 8, 3838–3847.
Saftig, P., Klumperman, J., 2009. Lysosome biogenesis and lysosomal membrane proteins: trafficking meets function. Nat. Rev. Mol. Cell Biol. 10, 623–635.
Saftig, P., Schroder, B., Blanz, J., 2010. Lysosomal membrane proteins: life between acid and neutral conditions. Biochem. Soc. Trans. 38, 1420–1423.
Sahani, M.H., Itakura, E., Mizushima, N., 2014. Expression of the autophagy substrate SQSTM1/p62 is restored during prolonged starvation depending on transcriptional upregulation and autophagy-derived amino acids. Autophagy 10, 431–441.
Salaun, B., de Saint-Vis, B., Clair-Moninot, V., Pin, J.J., Barthelemy-Dubois, C., Kissenpfennig, A., Peronne, C., Bates, E., Mattei, M.G., Lebecque, S., 2003. Cloning and characterization of the mouse homologue of the human dendritic cell maturation marker CD208/DC-LAMP. Eur. J. Immunol. 33, 2619–2629.
Salaun, B., de Saint-Vis, B., Pacheco, N., Pacheco, Y., Riesler, A., Isaac, S., Leroux, C., Clair-Moninot, V., Pin, J.J., Griffith, J., Treilleux, I., Goddard, S., Davoust, J., Kleijmeer, M., Lebecque, S., 2004. CD208/dendritic cell-lysosomal associated membrane protein is a marker of normal and transformed type II pneumocytes. Am. J. Pathol. 164, 861–871.
Subramaniam, M., Kern, B., Vogel, S., Klose, V., Schneider, G., Roeper, J., 2014. Selective increase of in vivo firing frequencies in DA SN neurons after proteasome inhibition in the ventral midbrain. Eur J Neurosci.
Tanaka, Y., Guhde, G., Suter, A., Eskelinen, E.L., Hartmann, D., Lullmann-Rauch, R., Janssen, P.M., Blanz, J., von Figura, K., Saftig, P., 2000. Accumulation of autophagic vacuoles and cardiomyopathy in LAMP-2-deficient mice. Nature 406, 902–906.
Tang, B., Cai, J., Sun, L., Li, Y., Qu, J., Snider, B.J., Wu, S., 2014. Proteasome inhibitors activate autophagy involving inhibition of PI3K-Akt-mTOR pathway as an anti-oxidation defense in human RPE cells. PLOS ONE 9, e103364.
Thal, D.R., Rub, U., Orantes, M., Braak, H., 2002. Phases of A beta-deposition in the human brain and its relevance for the development of AD. Neurology 58, 1791–1800.
Vogl, D.T., Stadtmauer, E.A., Tan, K.S., Heitjan, D.F., Davis, L.E., Pontiggia, L., Rangwala, R., Piao, S., Chang, Y.C., Scott, E.C., Paul, T.M., Nichols, C.W., Porter, D.L., Kaplan, J., Mallon, G., Bradner, J.E., Amaravadi, R.K., 2014. Combined autophagy and proteasome inhibition: a phase 1 trial of hydroxychloroquine and bortezomib in patients with relapsed/refractory myeloma. Autophagy 10, 1380–1390.
Wilke, S., Krausze, J., Bussow, K., 2012. Crystal structure of the conserved domain of the DC lysosomal associated membrane protein: implications for the lysosomal glycocalyx. BMC Biol. 10, 62.
Zang, Y., Thomas, S.M., Chan, E.T., Kirk, C.J., Freilino, M.L., DeLancey, H.M., Grandis, J.R., Li, C., Johnson, D.E., 2012. The next generation proteasome inhibitors carfilzomib and oprozomib activate prosurvival autophagy via induction of the unfolded protein response and ATF4. Autophagy 8, 1873–1874.